



# New series of quinazolinone derived Schiff's bases: synthesis, spectroscopic properties and evaluation of their antioxidant and cytotoxic activity

Zuzana Hricovíniová<sup>1</sup> · Michal Hricovíni<sup>2</sup> · Katarína Kozics<sup>3</sup>

Received: 7 August 2017 / Accepted: 18 November 2017 / Published online: 29 November 2017  
© Institute of Chemistry, Slovak Academy of Sciences 2017

## Abstract

A series of novel 2,3-di-substituted-2,3-dihydro-quinazolin-4(1*H*)-one derived Schiff's bases (**1–7**) have been designed, synthesized and characterized on the basis of their physical and spectral data. The presented microwave-assisted, phosphomolybdic acid (PMoA) catalysed, protocol provides an efficient and convenient route for the synthesis of structurally diverse and potentially biologically active compounds. The molecular structures of these Schiff's bases related to quinazolinones were confirmed by various spectroscopic methods (NMR, FTIR, UV–Vis) and their antioxidant activities were evaluated by UV–Vis and EPR spectroscopy employing 2,2'-azino-bis(3-ethylbenzothiazoline-6-sulphonic acid) (ABTS) assay. Derivatives **1–7** were examined for their cytotoxicity in vitro against human hepatocellular carcinoma cells (HepG2) using 3-(4,5-dimethylthiazol-2-yl)-2,5-diphenyltetrazolium bromide (MTT) assay. The structure–activity relationships study revealed that the position and nature of functional groups attached to the quinazolinone moiety alter their physico-chemical and biological properties. Derivatives **5**, **6** and **7** bearing multiple electron-donating groups were found to be the most active members of this series.

**Keywords** Quinazolinones · Heterogeneous catalysis · NMR · EPR spectroscopy · Antioxidant · Cytotoxic effect

## Introduction

Schiff's bases related to quinazolinones have been the subject of ongoing interest in medicinal field. Schiff's bases, also known as azomethines, possess potent biological activities and have been explored for their remarkable versatility (Schiff 1864; Sztanke et al. 2013). Their chemical and biological significance arises from the presence of

a lone electron pair in the  $sp^2$  hybridized orbital of the nitrogen atom. The mechanism of action likely proceeds through the hydrogen bond formation between the azomethine groups at the active centres of cellular entities (Zoubi 2013). An azomethine group (C=N) has been observed in several natural, natural product-derived, and synthetic compounds (Guo et al. 2007; Ernst et al. 2014; Zhang et al. 2016). Heterocyclic compounds of this group, depending on their molecular structure, have many possibilities for chemical permutation and can exhibit antimicrobial, antifungal, antitubercular, antiviral, anticancer, anticonvulsant and many other properties (Przybylski et al. 2009; Da Silva et al. 2011; Zoubi 2013). Moreover, Schiff's bases belong to an important class of nitrogen donor ligands and their metal complexes are used in pharmaceuticals for cancer targeting (Cozz 2004). Compounds with a quinazolinone skeleton isolated from plants and microorganisms (e.g. peganine, febrifugine, isofebrifugine, luotonin, bouchardatine) have been the subject of considerable interest due to their important therapeutic effects (Michael 2005; Mhaske and Argade 2006; Rakesh et al. 2015). Consequently, considerable effort has been directed towards the

**Electronic supplementary material** The online version of this article (<https://doi.org/10.1007/s11696-017-0345-y>) contains supplementary material, which is available to authorized users.

✉ Zuzana Hricovíniová  
Zuzana.Hricoviniova@savba.sk

<sup>1</sup> Institute of Chemistry, Slovak Academy of Sciences, 845 38 Bratislava, Slovakia

<sup>2</sup> Faculty of Chemical and Food Technology, Institute of Physical Chemistry and Chemical Physics, Slovak University of Technology, 812 37 Bratislava, Slovakia

<sup>3</sup> Cancer Research Institute, Biomedical Research Center, Slovak Academy of Sciences, 845 05 Bratislava, Slovakia

study of new quinazolinone derivatives due to their diverse pharmacological properties. A number of new derivatives and their complexes have been synthesised and their properties extensively investigated, including their chemistry, molecular structure, biological activities, and applications in various fields (Sawant et al. 2009; Khan et al. 2010; Chawla and Batra 2013; Rakesh et al. 2015). Recently, quinazolinone chemistry has undergone rapid development because of its extensive potential in medicinal chemistry and its relevance to cancer chemotherapy (Zahedifard et al. 2015). Derivatives which displayed considerable antioxidant properties were screened for their DNA protective activity (Kuntikana et al. 2016). The properties of quinazolinone derivatives vary considerably with even minor modifications in their molecular structure. Introduction of substituents together with their specific positions in the aromatic ring determine whether they behave as antioxidants, cytotoxic or mutagenic agents (Gawad et al. 2010; Kumar et al. 2011).

In the current context of sustainability, there is a growing demand for development of more efficient synthetic strategies, which can involve improvement in selectivity, elimination of hazardous chemicals, recovery, and reuse of reagents. Exploration of alternative green technologies in the synthesis of quinazolinone-derived Schiff's bases (the use of metallic or non-metallic catalysts, mechanochemical, ultrasonic or microwave activation) led to the development of novel efficient synthetic protocols (Martins et al. 2009; Wang et al. 2011; Zhang et al. 2016; Kuntikana et al. 2016). However, there is still a need to develop economical and environmentally friendly routes to obtain the desired compounds. Recently, solid heteropoly acids (HPA) have received a significant attention as they exhibit high catalytic activity and selectivity. HPA possess high Brønsted acidity and show higher catalytic activity than mineral acids but, at the same time, they are environmentally friendly, low in toxicity, non-corrosive, and economically cost effective (Kozhevnikov 1998; Firouzabadi and Jafari 2005). Applications of HPA in combination with unconventional energy sources have markedly improved the traditional methods of organic synthesis. Microwave irradiation (MW), as a clean energy source, has gained acceptance as an efficient tool and environmentally friendly technique (Loupy 2006).

Taking into consideration the wide range of applications of quinazolinone-based compounds in the field of pharmaceutical chemistry, we decided to synthesize a new series of quinazolinone-derived Schiff's bases. We wish to demonstrate that phosphomolybdic acid, supported on silica gel (PMoA/SiO<sub>2</sub>), could act as an efficient catalyst for their preparation. Herein we report the microwave-assisted and PMoA-catalysed synthesis, structural analysis, radical scavenging capacity and evaluation of the antiproliferative

potential of new 2,3-di-substituted-2,3-dihydro-quinazolin-4(1*H*)-ones aiming at potentially useful anticancer agents.

## Experimental

### Materials and methods

All chemicals were of reagent grade and used without further purification. High-resolution NMR spectra were recorded in a 5 mm cryoprobe at 25 °C on a Bruker Avance III HD spectrometer, at 14 T in DMSO-d<sub>6</sub>. The proton and carbon chemical shifts were referenced to TMS. One-dimensional 600 MHz <sup>1</sup>H and 150 MHz <sup>13</sup>C NMR spectra as well as two-dimensional COSY, HSQC and HMBC were used for determination of <sup>1</sup>H and <sup>13</sup>C chemical shifts. Chemical shifts ( $\delta$ ) are quoted in ppm and spin–spin coupling constants ( $J$ ) in Hertz. FT-IR spectra were measured on a Nicolet 6700 spectrometer (Thermo Fisher Scientific) with DTGS detector and OMNIC 8.0 software using 128 scans at the resolution of 4 cm<sup>-1</sup> with diamond ATR technique. Melting points were determined on a Kofler hot stage and are uncorrected. HRMS were acquired on an Orbitrap Velos PRO (Thermo Scientific), with electrospray ionization method, operated in positive mode. Microwave reactions were performed in a multimode microwave reactor CEM Discover consisting of a continuously focused microwave power delivery system with an operator-selectable power of 0–300 W and a microwave frequency source of 2.45 GHz. The progress of the reactions was monitored by thin layer chromatography (TLC) on aluminium sheets pre-coated with Silica Gel 60 F<sub>254</sub> (Merck). Solvent A (ethyl acetate/n-hexane/methanol 7:1:2 v/v/v); solvent B (ethyl acetate/chloroform/methanol 1:1:0.5 v/v/v).

### Determination of antioxidant activity

UV/Vis measurements were performed by means of a UV/Vis spectrometer (Shimadzu UV-3600) at 25 °C. The solution of semi-persistent free radical cation ABTS<sup>•+</sup> was prepared by dissolving of 2,2'-azino-bis(3-ethylbenzothiazoline-6-sulfonate diammonium salt), (ABTS, Sigma-Aldrich) and potassium persulfate in distilled water and storing in the dark for 16 h before use (Walker and Everette 2009). The stock solution of ABTS<sup>•+</sup> was prepared by dilution of the stored solution (1 ml) with 60 ml of distilled water to an overall concentration of 75  $\mu$ M (Re et al. 1999). The ABTS<sup>•+</sup> solution was mixed with 100  $\mu$ l of the sample solutions (DMSO, 1 mM) to a total volume of 3 ml (30:1 v/v) before the measurement. The antioxidant capacity of the studied compounds 1–7 was monitored by EPR spectroscopy on EPR spectrometer Bruker EMX Plus, using the ABTS<sup>•+</sup> free radical. A water-soluble analogue of vitamin E (Trolox, 6-hydroxy-2,5,7,8-tetramethylchroman-2-carboxylic acid,

Sigma-Aldrich) was used as an antioxidant standard. The solution of ABTS<sup>•+</sup> (67 μM) with a total volume of 1000 μl was added to one syringe. The samples (1 mM) dissolved in DMSO were transferred to the second syringe and measured under identical conditions as during the UV/Vis experiments. After simultaneous injection of both solutions into the cell (WG-814-Q, Wilmad LabGlass), the radical concentration was monitored for 5 min. The EPR spectra were recorded and evaluated using WinEPR (Bruker) software. Calculations and plots were processed using OriginPro 2016 (OriginLab).

### Cytotoxicity screening assay

The in vitro cytotoxicity screening was assessed using a malignant human hepatocellular cell line (HepG2) obtained from Prof. A. R. Collins (University of Oslo). The cells were cultured in RPMI 1640 medium supplemented with 10% fetal calf serum and antibiotics (penicillin 200 U/ml, streptomycin 100 μg/ml, kanamycin 100 μg/ml) on Petri dishes at 37 °C in humidified atmosphere of 5% CO<sub>2</sub>. The cytotoxicity of compounds **1–7** was monitored by MTT cell proliferation assay (Mosmann 1983; Berridge et al. 2005). In this assay the yellow tetrazolium salt MTT (3-(4,5-dimethylthiazol-2-yl)-2,5-diphenyltetrazolium bromide) is reduced by metabolically active cells to purple formazan that can be spectrophotometrically quantified. HepG2 cells were seeded into a set of 96 well plates at a density of 2 × 10<sup>4</sup>/well, and cultured in the RPMI 1640 medium. Exponentially growing cells were then pre-incubated in the presence of different concentrations of the tested compounds (1, 2, 5, 10, 20, 50, 120, 240, 480 μg/ml) for 24 h. Stock solutions of the tested samples **1–7** (96 mg/ml) in DMSO, and serial dilutions thereof, were prepared before the particular experiment. Cells treated with the medium only served as a negative control. After the treatment with **1–7**, the properly treated HepG2 cells were incubated in 100 μl of complete RPMI medium and

50 μl of 1 mM MTT solution for 4 h. After incubation, the MTT solution was removed, the formazan crystals in each well dissolved in DMSO (100 μl) and placed on an orbital shaker for 30 min. The absorbance intensity was measured using an xMark™ Microplate Spectrophotometer (Bio-Rad Lab) at 540 nm with a reference wavelength of 690 nm. All experiments were performed in triplicate, and the relative cell cytotoxicity was expressed as a percentage relative to the untreated control cells.

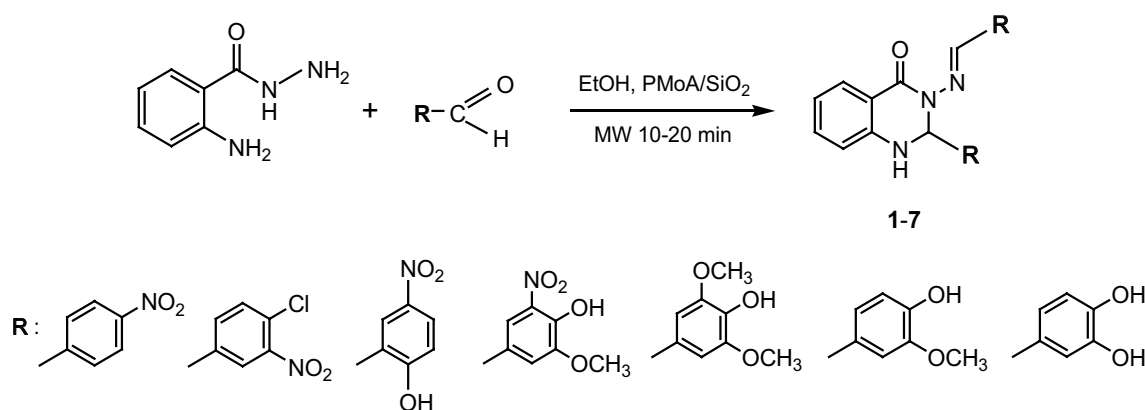
### Synthesis and spectral data

#### General procedure for the synthesis of 2,3-disubstituted-2,3-dihydro-quinazolin-4-one derived Schiff's bases under conventional conditions

A solution of 2-aminobenzhydrazide (ABH, 1 mmol) and the corresponding aromatic aldehyde (2 mmol) in dry ethanol (30 ml), in the presence of a catalytic amount of PMoA/SiO<sub>2</sub> (0.06 mmol, based on PMoA) (Hricovíniová 2016) was refluxed for 3–6 h. The progress of the reaction was checked by TLC and the composition of the reaction mixture was determined by <sup>1</sup>H NMR spectroscopy. The catalyst was filtered, washed with a small amount of ethanol, and dried. The reaction mixture was concentrated to syrup and the crude product thus obtained was purified by recrystallization (Scheme 1).

#### General procedure for the synthesis of 2,3-disubstituted-2,3-dihydro-quinazolin-4-one derived Schiff's bases under microwave-assisted conditions

A solution of ABH (1 mmol) and the corresponding aromatic aldehyde (2 mmol) in dry ethanol (30 ml), in the presence of a catalytic amount of PMoA/SiO<sub>2</sub> (0.06 mmol, based on PMoA) (Hricovíniová 2016) was mixed in a Pyrex glass tube and sealed with a Teflon septum. The reaction mixture



**Scheme 1** Microwave-assisted, PMoA-catalysed synthesis of Schiff's bases **1–7**

was exposed to microwave irradiation (200 W) for an appropriate time (5–20 min). Samples (0.5 ml) were measured at selected intervals and the composition of the reaction mixture was determined by  $^1\text{H}$  NMR spectroscopy. The PMoA/SiO<sub>2</sub> catalyst from the reaction mixture was filtered off. The desired products **1–7** were obtained using the same work-up procedure as listed for the conventional approach.

### 3-((4-nitrobenzylidene)amino)-2-(4-nitrophenyl)-2,3-dihydroquinazolin-4(1H)-one (**1**)

Yellow solid; yield 94.8%; m.p. 209–211 °C; Ref (Hricovíni and Hricovíni 2017) m.p. 207–208 °C; Ref (Fülöp et al. 1992) m.p. 215–217 °C;  $R_f$  0.78 (solvent A); FT-IR (ATR, diamond):  $\nu_{\text{max}}$ : 3380 (N–H), 3110 (C–H)<sub>Ar</sub>, 1648 (C=O), 1608 (HC=N), 1335, 1333 (NO<sub>2</sub>), 1290 (N–N) cm<sup>-1</sup>; UV–Vis (DMSO):  $\lambda_{\text{max}}$  344 nm; HRMS for C<sub>21</sub>H<sub>15</sub>N<sub>5</sub>O<sub>5</sub>Na: calcd [M + Na]<sup>+</sup> 440.3641; found 440.3638;  $^1\text{H}$  NMR and  $^{13}\text{C}$  NMR were in agreement with those recently published (Hricovíni and Hricovíni 2017) and our data are shown for better comparison with the other quinazolinone derivatives.  $^1\text{H}$  NMR (DMSO-d<sub>6</sub>, 600 MHz)  $\delta$ : 9.092 (s, 1H, N=C–H), 8.296 (d,  $J$  = 8.8 Hz, 2H, H-3", H-5"), 8.230 (d,  $J$  = 8.9 Hz, 2H, H-3', H-5'), 8.154 (d,  $J$  = 3.4 Hz, 1H, N–H), 7.968 (d,  $J$  = 8.8 Hz, 2H, H-2", H-6"), 7.748 (d,  $J$  = 7.5 Hz, 1H, H-5), 7.637 (d,  $J$  = 8.9 Hz, 2H, H-2', H-6'), 7.350 (dd,  $J$  = 8.6 Hz,  $J$  = 6.8 Hz, 1H, H-7), 6.853 (d,  $J$  = 8.2 Hz, 1H, H-8), 6.787 (dd,  $J$  = 7.5 Hz,  $J$  = 6.8 Hz, 1H, H-6), 6.763 (d,  $J$  = 3.4 Hz, 1H, H-2);  $^{13}\text{C}$  NMR (DMSO-d<sub>6</sub>, 150 MHz)  $\delta$ : 160.61 (C=O), 148.12 (C-4"), 147.91 (=CH), 147.48 (C-4'), 146.95 (C-1"), 145.81 (C-8a), 140.71 (C-1"), 134.62 (C-7), 128.32 (C-5), 128.22 (C-6"), 128.22 (C-2"), 127.63 (C-6'), 127.63 (C-2'), 124.06 (C-5"), 124.06 (C-3"), 123.79 (C-5'), 123.79 (C-3'), 118.45 (C-6), 115.14 (C-8), 114.41 (C-4a), 71.03 (C-2).

### 3-((4-chloro-3-nitrobenzylidene)amino)-2-(4-chloro-3-nitrophenyl)-2,3-dihydroquinazolin-4(1H)-one (**2**)

Light yellow solid; yield 90.4%; m.p. 211–213 °C;  $R_f$  0.74 (solvent A); FT-IR (ATR, diamond):  $\nu_{\text{max}}$ : 3377 (N–H), 3103 (C–H)<sub>Ar</sub>, 1650 (C=O), 1529 (HC=N), 1353 (NO<sub>2</sub>), 1299 (N–N), 1149 (C–N); 808 (C–Cl) cm<sup>-1</sup>; UV–Vis (DMSO):  $\lambda_{\text{max}}$  304, 364 nm; HRMS for C<sub>21</sub>H<sub>13</sub>Cl<sub>2</sub>N<sub>5</sub>O<sub>5</sub>Na: calcd [M + Na]<sup>+</sup> 509.2542; found 509.2546;  $^1\text{H}$  NMR (DMSO-d<sub>6</sub>, 600 MHz)  $\delta$ : 9.068 (s, 1H, N=C–H), 8.353 (d,  $J$  = 1.9 Hz, 1H, H-2"), 8.128 (d,  $J$  = 2.2 Hz, 1H, H-2'), 8.081 (d,  $J$  = 3.2 Hz, 1H, N–H), 8.018 (d,  $J$  = 8.5 Hz,  $J$  = 1.9 Hz, 1H, H-6"), 7.866 (d,  $J$  = 8.5 Hz, 1H, H-5"), 7.772 (d,  $J$  = 8.6 Hz, 1H, H-5'), 7.751 (dd,  $J$  = 7.7 Hz,  $J$  = 1.2 Hz, 1H, H-5), 7.598 (d,  $J$  = 8.6 Hz,  $J$  = 2.2 Hz, 1H, H-6'), 7.370 (ddd,  $J$  = 8.2 Hz,  $J$  = 7.4 Hz,  $J$  = 1.2 Hz, 1H, H-7), 6.855 (d,

$J$  = 8.2 Hz, 1H, H-8), 6.811 (dd,  $J$  = 8.2 Hz,  $J$  = 7.4 Hz, 1H, H-6), 6.675 (d,  $J$  = 3.2 Hz, 1H, H-2);  $^{13}\text{C}$  NMR (DMSO-d<sub>6</sub>, 150 MHz)  $\delta$ : 160.53 (C=O), 147.83 (C-3"), 147.76 (=CH), 147.38 (C-3'), 145.65 (C-8a), 140.81 (C-1'), 135.07 (C-1"), 134.68 (C-7), 132.29 (C-5"), 132.01 (C-5'), 131.82 (C-6"), 131.39 (C-6'), 128.32 (C-5), 126.31 (C-4"), 125.14 (C-4'), 123.90 (C-2'), 123.76 (C-2"), 118.62 (C-6), 115.17 (C-8), 114.35 (C-4a), 70.73 (C-2).

### 3-((2-hydroxy-5-nitrobenzylidene)amino)-2-(2-hydroxy-5-nitrophenyl)-2,3-dihydroquinazolin-4(1H)-one (**3**)

Yellow solid; yield 96.9%; m.p. 247–249 °C; Ref (Zahedifard et al. 2015) m.p. 250–252 °C;  $R_f$  0.61 (solvent A); UV–Vis (DMSO):  $\lambda_{\text{max}}$  298, 427 nm; HRMS for C<sub>21</sub>H<sub>15</sub>N<sub>5</sub>O<sub>7</sub>Na: calcd [M + Na]<sup>+</sup> 472.3629; found 472.3631; analytical data ( $^1\text{H}$  NMR,  $^{13}\text{C}$  NMR, FT-IR) were in agreement with those recently published (Zahedifard et al. 2015). Our  $^1\text{H}$  NMR and  $^{13}\text{C}$  NMR data are shown for better comparison with other quinazolinone derivatives.  $^1\text{H}$  NMR (DMSO-d<sub>6</sub>, 600 MHz)  $\delta$ : 8.825 (s, 1H, N=C–H), 8.442 (d,  $J$  = 2.9 Hz, 1H, H-6"), 8.159 (dd,  $J$  = 9.2 Hz,  $J$  = 2.9 Hz, 1H, H-4"), 8.107 (d,  $J$  = 9.2 Hz,  $J$  = 2.9 Hz, 1H, H-4'), 7.879 (d,  $J$  = 2.9 Hz, 1H, H-6'), 7.824 (d,  $J$  = 7.9 Hz, 1H, H-5), 7.697 (d,  $J$  = 2.5 Hz, 1H, N–H), 7.336 (dd,  $J$  = 8.3 Hz,  $J$  = 6.7 Hz, 1H, H-7), 7.101 (d,  $J$  = 9.2 Hz, 1H, H-3"), 7.086 (d,  $J$  = 9.2 Hz, 1H, H-3'), 6.849 (mult., 1H, H-8), 6.841 (mult., 1H, H-2), 6.796 (dd,  $J$  = 7.9 Hz,  $J$  = 6.7 Hz, 1H, H-6);  $^{13}\text{C}$  NMR (DMSO-d<sub>6</sub>, 150 MHz)  $\delta$ : 162.73 (C-6"), 161.67 (C-6'), 160.40 (C=O), 146.64 (=CH), 145.96 (C-8a), 139.82 (C-1"), 139.14 (C-1'), 134.60 (C-7), 128.18 (C-5), 126.86 (C-4"), 126.38 (C-4'), 125.10 (C-3'), 124.73 (C-2"), 122.21 (C-2'), 119.45 (C-3"), 118.11 (C-6), 117.36 (C-5"), 116.38 (C-5'), 114.98 (C-8), 113.14 (C-4a), 66.41 (C-2).

### 3-((4-hydroxy-3-methoxy-5-nitrobenzylidene)amino)-2-(4-hydroxy-3-methoxy-5-nitrophenyl)-2,3-dihydroquinazolin-4(1H)-one (**4**)

Orange solid; yield 77.4%; m.p. 225–227 °C;  $R_f$  0.74 (solvent A); FT-IR (ATR, diamond):  $\nu_{\text{max}}$ : 3497 (O–H), 3281 (C–H)<sub>Ar</sub>, 3083 (N–H), 1662 (C=O), 1543 (HC=N), 1262 (N–N), 1143 (C–N), 1101 (C–O), 1383 (NO<sub>2</sub>), 1059 (O–CH<sub>3</sub>) cm<sup>-1</sup>; UV–Vis (DMSO):  $\lambda_{\text{max}}$  365, 455 nm; HRMS for C<sub>23</sub>H<sub>19</sub>N<sub>5</sub>O<sub>9</sub>Na: calcd [M + Na]<sup>+</sup> 532.4148; found 532.4135;  $^1\text{H}$  NMR (DMSO-d<sub>6</sub>, 600 MHz)  $\delta$ : 10.959 (s, 1H, OH"), 10.572 (s, 1H, OH'), 8.877 (s, 1H, N=C–H), 7.873 (d,  $J$  = 2.3 Hz, 1H, N–H), 7.806 (d,  $J$  = 1.3 Hz, 1H, H-6"), 7.741 (d,  $J$  = 7.8 Hz, 1H, H-5), 7.559 (d,  $J$  = 1.3 Hz, 1H, H-2"), 7.401 (m, 2H, H-6', H-2'), 7.346 (dd,  $J$  = 8.2 Hz,  $J$  = 7.8 Hz, 1H, H-7), 6.839 (d,  $J$  = 8.2 Hz, 1H, H-8), 6.788

(t,  $J = 7.8$  Hz, 1H, H-6), 6.462 (d,  $J = 2.3$  Hz, 1H, H-2), 3.904 (s, 3H, OMe'), 3.821 (s, 3H, OMe'');  $^{13}\text{C}$  NMR (DMSO- $d_6$ , 150 MHz)  $\delta$ : 160.66 (C=O), 150.67 (=CH), 149.78 (C-3''), 149.54 (C-3'), 146.10 (C-8a), 144.49 (C-4''), 142.74 (C-4'), 137.10 (C-5''), 136.35 (C-5'), 134.24 (C-7), 130.25 (C-1'), 128.13 (C-5), 125.02 (C-1''), 118.23 (C-6), 116.26 (C-6''), 114.87 (C-8), 114.57 (C-6', C-2'), 113.84 (C-4a), 112.54 (C-2''), 71.56 (C-2), 56.59 (OMe'), 56.52 (OMe'').

### 3-((4-hydroxy-3,5-dimethoxybenzylidene)amino)-2-(4-hydroxy-3,5-dimethoxyphenyl)-2,3-dihydroquinazolin-4(1H)-one (5)

Light yellow solid; yield 66.9%; m.p. 175–176 °C;  $R_f$  0.69 (solvent B); FT-IR (ATR, diamond):  $\nu_{\text{max}}$ : 3507 (O–H), 3380 (N–H), 3117 (C–H)<sub>Ar</sub>, 1641 (C=O), 1609 (HC=N), 1250 (N–N), 1151 (C–N), 1111 (C–O), 1042 (O–CH<sub>3</sub>)  $\text{cm}^{-1}$ ; UV–Vis (DMSO):  $\lambda_{\text{max}}$  335 nm; HRMS for C<sub>25</sub>H<sub>25</sub>N<sub>3</sub>O<sub>7</sub>Na: calcd [M + Na]<sup>+</sup> 502.4717; found 502.4726;  $^1\text{H}$  NMR (DMSO- $d_6$ , 600 MHz)  $\delta$ : 8.714 (s, 1H, N=C–H), 7.968 (dd,  $J = 8.2$  Hz,  $J = 7.1$  Hz, 1H, H-7), 7.712 (d,  $J = 7.8$  Hz, 1H, H-5), 7.659 (s, 1H, N–H), 6.923 (s, 2H, H-2'' H-6''), 6.816 (d,  $J = 8.2$  Hz, 1H, H-8), 6.745 (dd,  $J = 7.8$  Hz,  $J = 7.1$  Hz, 1H, H-6), 6.704 (s, 2H, H-2', H-6'), 6.287 (s, 1H, H-2);  $^{13}\text{C}$  NMR (DMSO- $d_6$ , 150 MHz)  $\delta$ : 160.64 (C=O), 152.76 (=CH), 148.02 (C-3'', C-5''), 147.66 (C-3', C-5'), 146.45 (C-8a), 138.23 (C-4''), 135.72 (C-4'), 133.69 (C-7), 130.05 (C-1'), 127.86 (C-5), 124.61 (C-1''), 117.67 (C-6), 114.89 (C-4a), 114.61 (C-8), 104.90 (C-2'', C-6''), 104.61 (C-2', C-6'), 72.64 (C-2).

### 3-((4-hydroxy-3-methoxybenzylidene)amino)-2-(4-hydroxy-3-methoxyphenyl)-2,3-dihydroquinazolin-4(1H)-one (6)

Off white solid; yield 74.9%; m.p. 190–192 °C;  $R_f$  0.75 (solvent B); FT-IR (ATR, diamond):  $\nu_{\text{max}}$ : 3497 (O–H), 3281 (C–H)<sub>Ar</sub>, 3083 (N–H), 1662 (C=O), 1543 (HC=N), 1262 (N–N), 1143 (C–N), 1101 (C–O), 1383 (NO<sub>2</sub>), 1059 (O–CH<sub>3</sub>)  $\text{cm}^{-1}$ ; UV–Vis (DMSO):  $\lambda_{\text{max}}$  332 nm; HRMS for C<sub>23</sub>H<sub>21</sub>N<sub>3</sub>O<sub>5</sub>Na: calcd [M + Na]<sup>+</sup> 442.4197; found 442.4192;  $^1\text{H}$  NMR (DMSO- $d_6$ , 600 MHz)  $\delta$ : 9.552 (s, 1H, O–H''), 9.033 (s, 1H, O–H'), 8.683 (s, 1H, N=C–H), 7.698 (d,  $J = 7.7$  Hz, 1H, H-5), 7.652 (d,  $J = 2.2$  Hz, 1H, N–H), 7.284 (dd,  $J = 8.1$  Hz,  $J = 7.3$  Hz, 1H, H-7), 7.265 (s, 1H, H-6''), 7.105 (d,  $J = 8.1$  Hz, 1H, H-2''), 7.056 (s, 1H, H-6'), 6.818 (d,  $J = 8.1$  Hz, 1H, H-3''), 6.788 (d,  $J = 8.1$  Hz, 1H, H-8), 6.735 (m, 2H, H-2', H-6), 6.672 (d,  $J = 8.2$  Hz, 1H, H-3'), 6.287 (d,  $J = 2.2$  Hz, 1H, H-2), 3.783 (s, 3H, OCH<sub>3</sub>''), 3.701 (s, 3H, OCH<sub>3</sub>');  $^{13}\text{C}$  NMR (DMSO- $d_6$ , 150 MHz)  $\delta$ : 160.57 (C=O), 153.12 (=CH), 149.25 (C-5''), 147.87 (C-4''), 147.42 (C-4'), 146.59 (C-5'), 146.31 (C-8a), 133.65 (C-7),

130.93 (C-1'), 127.88 (C-5), 125.81 (C-1''), 122.11 (C-2''), 118.98 (C-6), 117.57 (C-2'), 115.40 (C-3''), 114.88 (C-3'), 114.61 (C-8), 111.07 (C-6'), 109.67 (C-6''), 72.11 (C-2), 55.56 (OCH<sub>3</sub>''), 55.52 (OCH<sub>3</sub>').

### 3-((3,4-dihydroxybenzylidene)amino)-2-(3,4-dihydroxyphenyl)-2,3-dihydroquinazolin-4(1H)-one (7)

Off white solid; yield 65.8%; m.p. 201–203 °C;  $R_f$  0.57 (solvent B); FT-IR (ATR, diamond):  $\nu_{\text{max}}$ : 3421 (O–H), 3291 (N–H), 3067 (C–H)<sub>Ar</sub>, 1608 (C=O), 1514 (HC=N), 1281 (N–N), 1143 (C–N), 1115 (C–O)  $\text{cm}^{-1}$ ; UV–Vis (DMSO):  $\lambda_{\text{max}}$  302, 338 nm; HRMS for C<sub>21</sub>H<sub>17</sub>N<sub>3</sub>O<sub>5</sub>Na: calcd [M + Na]<sup>+</sup> 414.3666; found 414.3662;  $^1\text{H}$  NMR (DMSO- $d_6$ , 600 MHz)  $\delta$ : 9.280 (s, 2H, O–H(4)', O–H(4)''), 8.890 (s, 2H, O–H(3)', O–H(3)''), 8.530 (s, 1H, N=C–H), 7.686 (m, 1H, H-5), 7.682 (m, 1H, H-2') 7.602 (s, N–H), 7.262 (dd,  $J = 8.0$  Hz,  $J = 7.3$  Hz, 1H, H-7), 7.192 (s, 1H, H-2''), 6.926 (d,  $J = 8.1$  Hz, 1H, H-6''), 6.763 (m, H, H-8), 6.760 (m, 1H, H-5''), 6.707 (t, 1H,  $J = 8.0$  Hz,  $J = 7.1$  Hz, H-6), 6.640 (m, 2H, H-5', H-6'), 6.214 (s, 1H, H-2);  $^{13}\text{C}$  NMR (DMSO- $d_6$ , 150 MHz)  $\delta$ : 160.37 (C=O), 152.34 (=CH), 148.24 (C-3''), 146.06 (C-8a), 145.59 (C-3'), 145.30 (C-4'), 144.97 (C-4''), 133.56 (C-7), 131.49 (C-2'), 131.15 (C-1'), 127.89 (C-5), 125.84 (C-1''), 121.03 (C-6''), 117.44 (C-6), 117.35 (C-5'), 115.33 (C-8), 114.84 (C-4a), 113.77 (C-5''), 112.86 (C-2''), 71.51 (C-2).

## Results and discussion

### Chemistry

The first part of our work was aimed at the synthesis of Schiff's bases derived from the quinazolinone heterocyclic skeleton. We have focused on the development of a method that is simple, fast, and offers high yields of products. Schiff's bases are formed by condensation of the primary amines and structurally diverse aldehydes. The direct condensation reaction occurs at high temperatures and this thermal approach is very practical in many cases (Fülöp et al. 1992; Gawad et al. 2010). We decided to build on our previous experience in this field by exploring the effect of the reusable heterogeneous PMoA/SiO<sub>2</sub> catalyst and microwaves (Hricovíniová 2016) on the synthesis of a homologous series of quinazolin-4-one derived Schiff's bases.

Adjacent amino and hydrazino functional groups in heterocyclic compounds provide opportunities for construction of an additional ring system. Primary amines and aldehydes react under acid catalysis to form imine derivatives as the condensation products. The reaction is reversible and the formation of imine requires the presence of acid, which is necessary for subsequent elimination of water. Our attention

was aimed at the modification of the aryl moiety at positions 2 and 3 of the quinazolin-4-one scaffold to yield structural analogues with appreciable biological activity.

Acid hydrazides are useful intermediates for the synthesis of *N*-heterocyclic compounds. The procedure for building up such a heterocyclic system is based on the cyclization reaction in dry solvent. As shown in Scheme 1, acid-catalysed cyclocondensation of aromatic hydrazide with various aromatic aldehydes provided the corresponding 2,3-disubstituted-2,3-dihydro-quinazolin-4-ones. In a typical experiment, a mixture of 2-aminobenzhydrazide (ABH, 1.0 equiv.) and an aromatic aldehyde (2.0 equiv.) was dissolved in absolute ethanol, and, in the presence of acid catalyst, was refluxed in an oil-bath at 85 °C. After several hours, the crude product thus obtained was purified by recrystallization from an appropriate solvent. In this study, a new catalytic system based on phosphomolybdic acid supported on silica gel (PMoA/SiO<sub>2</sub>) has been tested. We screened the effect of different acid promoters by testing several acid catalysts. Experiments using glacial acetic acid, sulfuric acid, *p*-toluenesulfonic acid and PMoA/SiO<sub>2</sub> gave interesting results. We also examined whether MW irradiation could facilitate the cyclo condensation reaction to form the desired Schiff's bases. The effect of MW irradiation on conversion was explored using a multimode microwave reactor consisting of a continuous focus MW power delivery system with operator-selectable power. Preliminary results showed considerable improvements in Schiff's base formation when using MW irradiation compared to the conventional method. Both yields and the composition of the reaction mixtures depended on the length of exposure, as well as on the structure of the aromatic aldehyde. The thermal effects of irradiation arise from the dissipation of energy into heat as a result of intermolecular friction when the dipoles change their mutual orientation on the alternation of the electric field at a high frequency. Thus, MW irradiation caused a remarkable acceleration of the condensation reaction due to efficient energy transfer and, consequently, both the reaction kinetics and the yields markedly increased. The Schiff's base syntheses were carried out in a microwave reactor at a power of 200 W, and took around 10–20 min. The three-component reaction employing ABH, aromatic aldehyde and acid catalyst in ethanol proceeded smoothly, and all catalysts tested exhibited good activity. However, the cyclo condensation reaction proceeded most effectively in the presence of PMoA/SiO<sub>2</sub>. At the end of the reaction, the catalyst was recovered by simple filtration, washed with ethanol and dried at 160 °C for 2 h. The catalyst could be reused several times in the subsequent reaction without notable loss of activity. This approach yielded the required 2,3-disubstituted-quinazolinones in higher yields in considerably shorter times (Table 1). It should be noted that applying power exceeding 200 W did not improve the

**Table 1** Data of the microwave-assisted, PMoA-catalysed cyclocondensation reaction of ABH with variably substituted aromatic aldehydes

Schiff's base	Microwave field		Oil-bath heating	
	Time (min)	Yield %	Time (min)	Yield %
<b>1</b>	10	95	180	88
<b>2</b>	15	90	180	80
<b>3</b>	15	97	240	89
<b>4</b>	15	77	300	65
<b>5</b>	20	67	300	56
<b>6</b>	15	75	360	66
<b>7</b>	20	66	360	48

Conversions are also shown for conventional oil-bath heating to demonstrate the differences between microwave and conventional approaches

product yield. Experimental results clearly showed that MW irradiation increased the reaction rate (10–20 min) and the yield (66–97%) compared to conventional heating (3–6 h, yield 48–89%). Our experimental results are in agreement with recent developments in quinazolinone synthesis, where microwave irradiation has provided a major advantage over conventional thermal methods (Besson and Chosson 2007). The worth of microwave-assisted synthesis has been proven in spectacular acceleration of reaction times (reduced from hours to minutes), increased yields, decreased side-products, and simple reaction setup also in other organic reactions (Hricovíiová 2006, 2010, 2016).

### NMR spectral analysis

The structures of the new compounds were established by 1D and 2D NMR spectroscopic studies. The structural assignments based on the NMR, IR, and HRMS data are listed in the experimental part. High-resolution NMR spectral data confirmed the proposed structures of the synthesized compounds **1–7**. The chemical shifts and three-bond proton–proton coupling constants ( $^3J_{\text{H-H}}$ ) for H-5–H-8 were not much affected by substitution at the aromatic rings in the various compounds. Chemical shifts for these four protons varied by about 0.1 ppm for **1–7** in DMSO. The most deshielded one was H-5 (having chemical shifts close to 7.7 ppm in all seven derivatives) whereas H-6 resonated in the interval of 6.7–6.8 ppm. Slightly bigger variations in chemical shifts values were shown by azomethine and the N–H protons—both varied by about 0.4 ppm for **1–7**. The azomethine proton was most deshielded in **1** (9.09 ppm) and **2** (9.07 ppm) which contain nitro group (*para*- or *meta*-substituted) but have no substituent at the *ortho*- position in the ring. On the other hand, the presence of OH groups caused shielding of this proton resulting in lower values of

the chemical shift in **3** (8.83 ppm) and **7** (8.53 ppm). Protons in the NH or OH (in **3–7**) groups showed much higher variability in chemical shift values. The NH protons were most deshielded in **1** and **2** ( $\delta > 8$  ppm), while protons in all the other derivatives showed chemical shifts in the range of 7.6–7.9 ppm. As expected, the biggest variations in  $^1\text{H}$  chemical shifts were detected for OH groups. Intramolecular hydrogen bonds caused a strong increase of chemical shift values in **3** (12.341 and 11.936 ppm) whereas the shift values of the OH protons flanked by the two methoxy groups were considerably smaller in **5** (8.942 and 8.447 ppm). The presence of these methoxy groups at each of the aromatic rings thus strongly affected the shielding of these OH protons. Furthermore, the temperature dependence of the OH groups showed that the intramolecular H-bonds were competing with intermolecular hydrogen bonds with the solvent (Hricovíni and Hricovíni 2017). In **3** the H-bond was formed between the OH group and the nitrogen in the azomethine group.

The chemical shifts of protons at the two aromatic rings (one linked to C-2 and the second to the azomethine group) varied considerably upon substitution. The effects of the electron-withdrawing groups, such as the nitro group, were seen clearly in **2**, where the protons H-2' ( $\delta = 8.13$ ) and H-2'' ( $\delta = 8.35$  ppm) were considerably deshielded. This group also showed similar deshielding effects in **1** (for protons H-3', H-3'', H-5' and H-5'') and **4** (H-6''). On the other hand, the effect of introducing methoxy groups was lower chemical shifts values for the ring protons in **4** (H-2' and H-2'',  $\delta = 7.40$  ppm and  $\delta = 7.56$  ppm), in **5** (H-2', H-2'', H-6' and H-6'', all having  $\delta = 6.70$ – $6.99$  ppm) and in **6** (H-6' and H-6'',  $\delta = 7.06$  ppm and  $\delta = 7.27$  ppm). Obviously, the chemical shift values of the aromatic protons were also affected by the presence of other substituents (OH and Cl). Apart from the methoxy protons, the most shielded signal in **1–7** was that of the proton in the  $-\text{N}-\text{C}_2(\text{H})$  group which resonated between 6.21 and 6.85 ppm. Similarly, to proton chemical shifts, the carbon  $\delta$  values also varied for **1–7**. As expected, the carbonyl signal was most deshielded (approximately 160 ppm), and, apart from the methoxy groups present in **4–6** ( $\delta \sim 56$  ppm), the most shielded carbon was C-2 linked to two nitrogen atoms. The chemical shifts of the latter carbon varied between 70.73 and 72.11 ppm for all derivatives, except for **3**. The considerably lower  $\delta$  value detected for C-2 in **3** (66.41 ppm) is due to the effect of the OH group in the *ortho*- position in the two aromatic rings linked to C-2 and to the azomethine group. The  $^1\text{H}$  and  $^{13}\text{C}$  NMR spectra of derivative **4**, as representative of these compounds, is presented in Fig. 1.

## FT-IR spectra

The FT-IR spectra also provided valuable structural information on the synthesised compounds. Formation of the new quinazolin-4-one derived Schiff's bases **1–7** was inferred from the appearance of sharp absorption bands in the IR spectra due to the characteristic azomethine ( $\text{CH}=\text{N}$ ) stretch at  $1514$ – $1609$   $\text{cm}^{-1}$ . Moreover, the broad absorption bands observed in the spectra near  $3300$ – $3400$   $\text{cm}^{-1}$  could be attributed to the (N–H) stretching vibrations of the quinazoline ring. The  $\text{NO}_2$  group stretch in **1**, **2**, **3**, and **4** was confirmed by the presence of strong bands in the range of  $1333$ – $1383$   $\text{cm}^{-1}$ . The C–Cl (halogen) absorption frequency band appeared at  $808$   $\text{cm}^{-1}$  (**2**). Bands characteristic for the phenolic group (O–H) were observed at  $3366$ – $3507$   $\text{cm}^{-1}$  and the bands at approximately  $1650$   $\text{cm}^{-1}$  were assigned to the carbonyl groups (C=O).

## UV-Vis absorption spectra

We also used UV-Vis spectroscopy to study the electronic absorption spectra of the Schiff's bases **1–7**. DMSO solutions of the compounds were prepared at concentration of 0.1 mM and measured immediately after preparation. The individual absorption maxima ( $\lambda_{\text{max}}$ ), and extinction coefficients ( $\epsilon_{\text{max}}$ ) of **1–7** are given in Table 2. The differences between the derivatives, bearing various functional groups, are clearly visible from the individual maxima and the calculated values of the extinction coefficients. Compounds **2–4** and **7** showed two separated absorption maxima, with the first in the range of 300–370 nm and the second between 350 and 500 nm.

The excitations around 300 nm point to the presence of a C=N bond conjugated with the aromatic ring system. The absorption bands in the range from 330–350 nm can be attributed to  $\pi$ – $\pi^*$  transitions in systems where the phenyl rings are conjugated with the non-bonding pairs and the C=C double bonds. Such conjugation is typical for systems with substituents containing groups with non-bonding pairs, such as OH and NH groups. In the case of compound **1**, bearing the  $\text{NO}_2$  groups, the broad maximum is visible at 344 nm, belonging to the  $\pi$ – $\pi^*$  transitions of the phenyl systems. The non-bonding pairs contribute to the conjugation and are responsible for the relatively high absorbance. The same is seen for derivative **7**, which possesses only OH substituents, with  $\lambda_{\text{max}}$  at 338 nm ( $\pi$ – $\pi^*$  transitions) and 302 nm (azomethine conjugation with aromatic system). The differences among these compounds are caused by the different excited states arising from the varying type and position of the substituent (Blevins and Blanchard 2004). This results in a different distribution of electrons over the system, affecting the excitation energies (Crompton and Lewis 2004). The strong conjugation of the non-bonding electron pairs in the

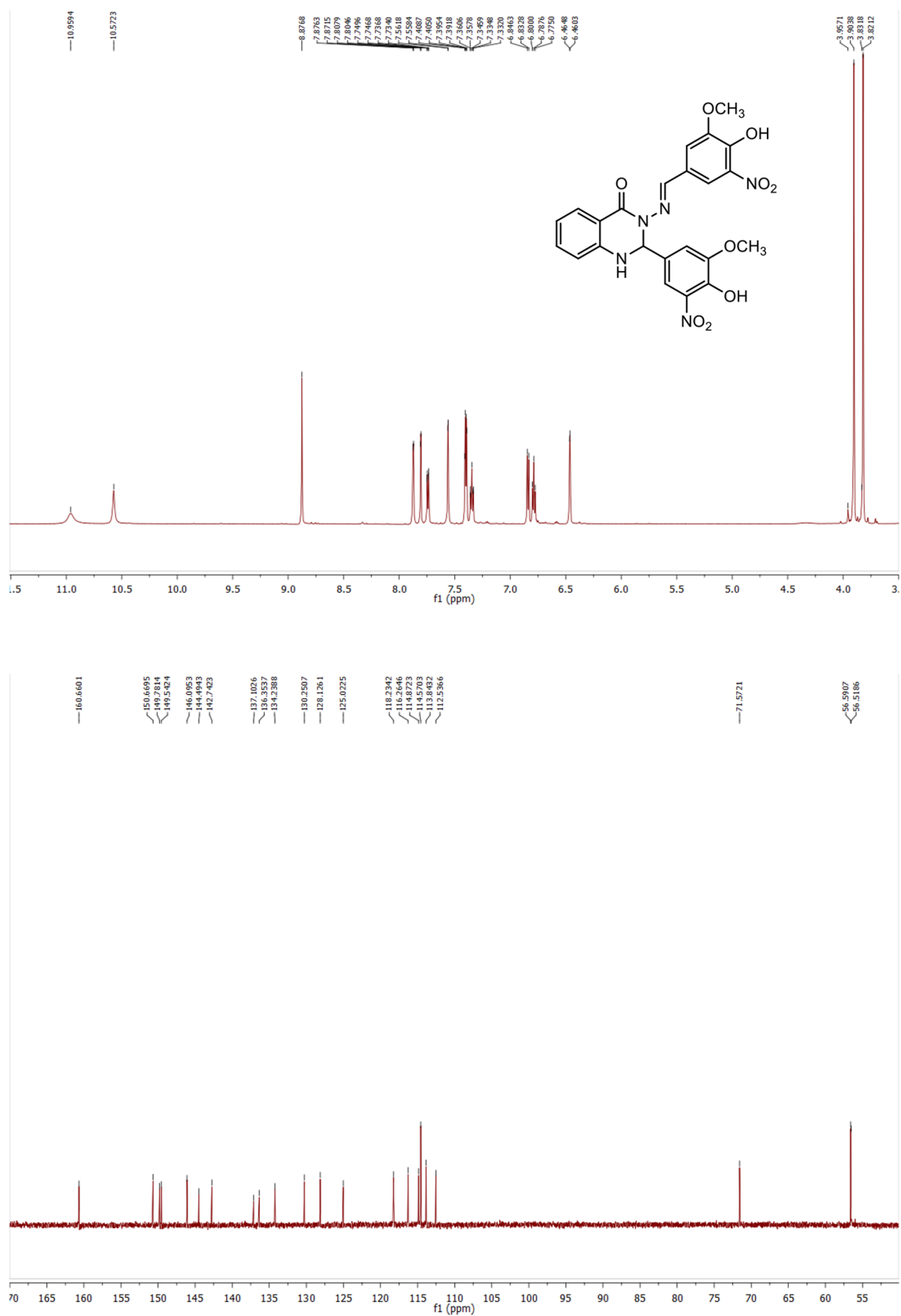


Fig. 1 <sup>1</sup>H and <sup>13</sup>C NMR spectra of compound 4



**Table 2** The absorption maxima and the extinction coefficients of Schiff's bases 1–7 in DMSO

Schiff's base	1	2	3	4	5	6	7
$\lambda_{\max}/\text{nm}$	344	304	298	365	335	332	302
$\epsilon_{\max}/\text{dm}^3 \text{ mol}^{-1} \text{ cm}^{-1}$	17860	15380	19700	15560	17040	17330	29210
		364	427	455			338
		7320	29700	3970			26700

OH groups, along with the positional effect of the substituents, results in high absorbance for compound **7** as seen from the high extinction coefficient values. On the other hand, **5** and **6** have similar spectra and the maxima are close to each other ( $\lambda_{\max}$  335 and 332 nm, respectively) due to their very similar structure, differing only in that **5** has two *para*-methoxy groups and **6** only one. Methoxy groups are less conjugated and have a slightly less intense substituent effect than the OH groups (Crompton and Lewis 2004), which results in lower absorbance of compounds. Spectrum of compound **4** is slightly shifted ( $\lambda_{\max}$  365 nm) due to the solvation effect of DMSO, associated with intramolecular hydrogen bonds causing a bathochromic shift of the maximum to a longer wavelength (Díaz et al. 2009). The absorption maxima in the range 350–500 nm correspond to the  $n-\pi^*$  transitions typical for chromophores ( $\text{N}=\text{N}$ ) and found in similar systems (Nielsen et al. 2006). The very strong absorption band of **3** and **4** ( $\lambda_{\max}$  427 nm for **3** and 455 nm for **4**, respectively) is caused by the auxochromic effect of  $\text{NO}_2$  coupled with the effect of the OH groups. Moreover, the solvation effect of DMSO molecules, as well as possible intramolecular hydrogen bonds, increases the bathochromic shift of the maximum to longer wavelengths, as seen previously for similar systems (Kaur et al. 2017). In the case of **2**, the effect of the  $\text{NO}_2$  group is diminished by the chlorine substituent, which has a very strong mesomeric effect and causes a redistribution of electrons in the aromatic rings. Consequently, the absorption maximum is there decreased to 364 nm and 304 nm (azomethine conjugation with aromatic system).

## Determination of antioxidant activity

### Radical scavenging properties investigated by UV/Vis spectroscopy

Antioxidant activity is directly related to the ability of compounds to release hydrogen atoms. The mechanism leading to elimination of free radicals is based on the donation of hydrogen to free radicals, reducing them to unreactive species (Halliwell et al. 1999). The characterisation of antioxidant properties by Trolox equivalent antioxidant capacity (TEAC) is a suitable approach for investigations of the radical-scavenging activity of compounds containing condensed aromatic ring systems (Re et al. 1999; Tian and Schaich 2013). A TEAC assay is based on the reaction of

semi-persistent radicals with the investigated molecules. The ABTS [2,2'-azino-bis(3-ethylbenzothiazoline-6-sulphonic acid)] salt was used as a source of the semi-stable radical cation ( $\text{ABTS}^{\bullet+}$ ). The antioxidant activity is determined by the decolourisation of the  $\text{ABTS}^{\bullet+}$  solution, i.e. the reduction of the radical cation is measured by its concomitant decrease in absorbance. The UV–Vis measurements for all investigated compounds were performed with aliquots of  $\text{ABTS}^{\bullet+}$  diluted to an absorbance of  $\sim 1.0$  at 735 nm. The kinetics of the reaction of  $\text{ABTS}^{\bullet+}$  with the studied compounds was monitored at a fixed wavelength (735 nm) for a 15 min period, which was found to be sufficient time to allow the system to reach a steady-state level. A significant drop in absorbance was observed in all samples (**1–7**) immediately after starting the measurements. The absorbance curves recorded during the reaction of  $\text{ABTS}^{\bullet+}$  with the selected Schiff's bases are shown in Fig. 2.

The results thus obtained indicated significant antioxidant activity for all compounds. The number and position of the aromatic hydroxyl groups is of crucial importance in modulating the antioxidant capacity. Electron-donating groups, especially alkyl and methoxy groups had previously been reported to increase the electron density of phenoxyl radicals, leading to enhancement of the radical scavenging and antioxidant activity (Kajiyama and Ohkatsu 2001; Kuntikana et al. 2016). The high activity of  $\alpha$ -tocopherol (vitamin E) was attributed to the *para*-alkoxy

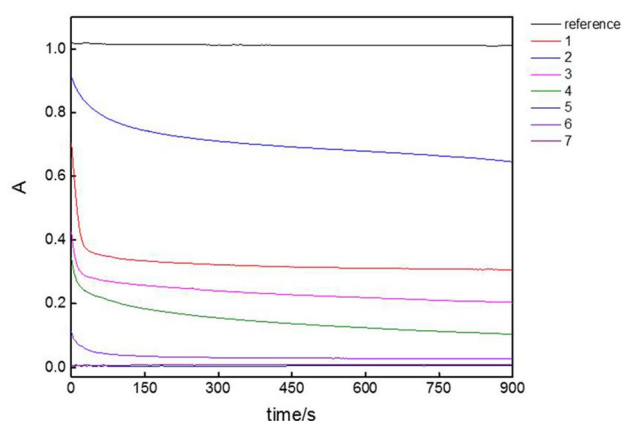


**Fig. 2** Time-dependent absorbance changes of  $\text{ABTS}^{\bullet+}$  at 735 nm, in the presence of Schiff's bases **1–7** in DMSO, compared to the reference solution (DMSO)

group and the methyl groups on the aromatic ring (Brees et al. 2000). The data clearly showed that compound **7**, bearing multiple hydroxyl groups, exhibited the highest quenching activity—the absorbance is a flat zero, indicating a quenching reaction so fast, it was over before recording could begin. Compound **5**, bearing four methoxy and two hydroxyl groups on the aromatic rings, showed very similar activity to that of **7**. The NH group present in the quinazolinone moiety also participates in the antioxidant activity, but its effect is minor compared to the radical scavenging activity of the OH or OCH<sub>3</sub> groups. Both derivatives thus manifested very high antioxidant activity, showing a massive initial absorbance drop with no further reaction thereafter. The reaction between ABTS<sup>•+</sup> and compound **6** showed a small decrease in antioxidant activity compared to **5** and **7**. The large initial drop in absorbance was followed by an ongoing slow decrease of the kinetic curve. This behaviour is typical for many small aromatic compounds containing multiple OH groups (or combined with an OCH<sub>3</sub> group) along with an aliphatic system, e.g. gallic acid and coniferyl alcohol (Walker and Everette 2009).

An interesting feature of this series of compounds is the effect of halogenation, methoxylation and nitration of aromatic rings. Replacement of a methoxy group with the electron-withdrawing nitro group (**4**) led to diminution of the antioxidant activity. The drop in absorbance showed a similar but more gradual trend. Removal of the methoxy group and variation of the position of the hydroxyl group (**3**) resulted in another reduction of the free radical quenching ability, caused by different electron distribution in the aromatic ring system. In this case, a smaller intense decrease at the start of recording was observed, followed by a slow decrease of the absorbance, but not as significant as seen for **4**. The complete absence of OH groups in compound (**1**) meant that the hydrogen of the NH group was the only one involved in the radical-scavenging reaction. In this case, there was a sharp initial drop at the start of recording, but very little change afterwards. Completely different behaviour was observed when a chlorine atom was present on the phenyl ring along with the nitro group (**2**). This curve looked rather different to others, with a far more leisurely initial absorbance drop, followed by gradual, steady decrease spanning over the whole measurement period.

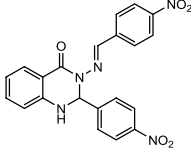
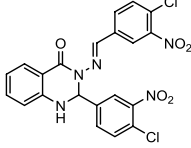
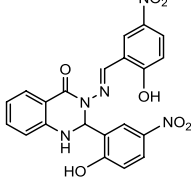
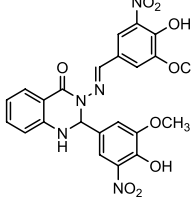
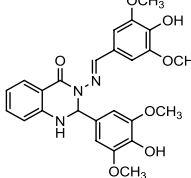
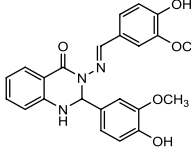
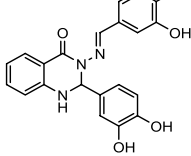
The antioxidant activity of a given compound is characterized by the TEAC value (Trolox equivalent antioxidant capacity):

$$\text{TEAC} = \frac{(A_f - A_0)_{\text{sample}}}{(A_f - A_0)_{\text{trolox}}}$$

where  $A_f$  is the final absorbance and  $A_0$  is the initial ABTS<sup>•+</sup> absorbance value of the sample or Trolox standard.

The decrease of ABTS<sup>•+</sup> concentration caused by the antioxidant action of the tested compounds can be calculated from the TEAC value, assuming that two ABTS<sup>•+</sup> molecules are eliminated by one Trolox molecule (Tian and Schlich 2013). The TEAC values of the studied Schiff's bases **1–7** are summarized in Table 3. The absorbance changes

**Table 3** The TEAC values of Schiff's bases **1–7** calculated from kinetic and EPR measurements

Schiff's base	Structure	TEAC <sub>ABTS-UV/vis</sub>	TEAC <sub>ABTS,EPR</sub>
<b>1</b>		0.87 ± 0.03	0.91 ± 0.02
<b>2</b>		0.51 ± 0.01	0.46 ± 0.01
<b>3</b>		0.98 ± 0.03	1.04 ± 0.03
<b>4</b>		1.09 ± 0.03	1.17 ± 0.03
<b>5</b>		1.19 ± 0.04	1.30 ± 0.04
<b>6</b>		1.17 ± 0.04	1.27 ± 0.03
<b>7</b>		1.21 ± 0.04	1.36 ± 0.04

observed in our data suggest that the molecular structure and steric accessibility to the hindered radical site in  $\text{ABTS}^{\bullet+}$  are the dominant factors controlling the reaction rates of our compounds with  $\text{ABTS}^{\bullet+}$ .

### Radical scavenging properties investigated by EPR spectroscopy

The antioxidant activity of the investigated Schiff's bases was also monitored via EPR spectroscopy. For this purpose, a set of experiments was performed with all compounds **1–7** using the  $\text{ABTS}^{\bullet+}$  radical. All the experiments were initiated by mixing a sample of compound dissolved in DMSO with a solution of  $\text{ABTS}^{\bullet+}$  in distilled water. Figure 3 presents the characteristic changes over time of the EPR spectra of five selected compounds.

The plots of the selected spectra over time show the decrease of the  $\text{ABTS}^{\bullet+}$  signal. No changes in the intensity of the EPR spectra were observed in the sample-free reference (Fig. 3).

When performed with the Schiff's bases, however, all of them showed clear changes in the  $\text{ABTS}^{\bullet+}$  concentrations over the period of the experiment (including **5** and **7**, not shown here). The double integral intensities of  $\text{ABTS}^{\bullet+}$  were evaluated for the time evolutions of all the experimental EPR spectra. The  $\text{ABTS}^{\bullet+}$  concentrations of individual samples and the reference were calculated and used for determination of the TEAC value. All data are summarized in Table 3 and

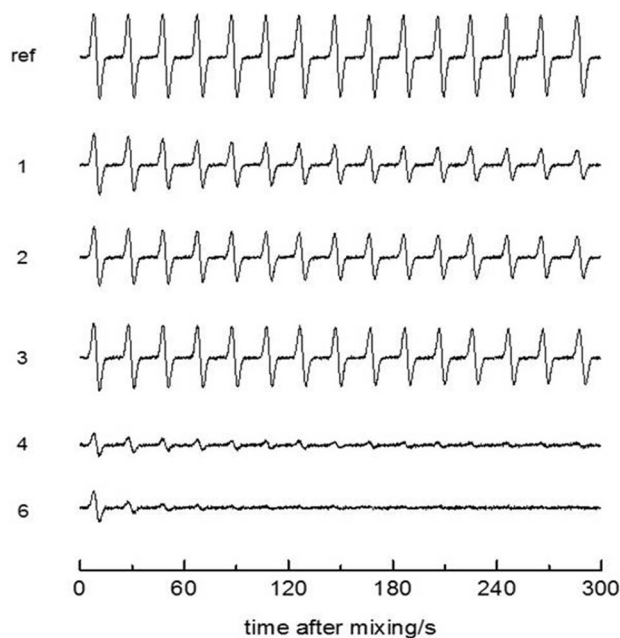


**Fig. 3** Evolution over time of the EPR signals recorded after mixing a solution of a Schiff's bases (**1–4** and **6**), or reference (DMSO), with a solution of the radical oxidant ( $\text{ABTS}^{\bullet+}$ )

are in good agreement with the kinetic experiments. The highest TEAC values were found for **5**, **6** and **7**, reflecting their high antioxidant activity, as seen in the individual spectra of **6** in Fig. 3. The spectra of compounds **3**, **4** and **6** were recorded with  $10 \times$  diluted samples with a concentration of  $1.10^{-4}$  M, to avoid signal extinction before the experiment could begin. It should also be noted that the signal intensities of **5** and **7** diminished quite rapidly during the recording period (even at  $1.10^{-4}$  M concentration) due to the fast extinction of the radicals. The EPR results thus confirmed the strong antioxidant properties of the investigated Schiff's bases antioxidants in the presence of radical  $\text{ABTS}^{\bullet+}$ . Minor differences (without any effect on the antioxidant activities of **1–7**) between the TEAC values obtained from the UV–Vis and EPR measurements were possibly caused by the different settings of the experiments. A minor delay arose between the mixing of the solutions and the start of measurement, due to transfer of the solution mixture from syringes to the cell in EPR spectrometer. Nevertheless, both experimental methods, UV–Vis and EPR, indicated all the investigated Schiff's bases to possess very good antioxidant properties, making them worthy of further study regarding their biological activity.

### Determination of cytotoxic activity

MTT assay is commonly used for the evaluation of cell proliferation and hence is a good indicator of cell death or inhibition of growth. The synthesized compounds **1–7** were subjected to the colorimetric MTT assay to be evaluated for their in vitro cytotoxicity against the malignant human hepatocellular HepG2 cell line. HepG2 was chosen because these cells are used as a model system for studies of liver metabolism and toxicity of xenobiotics, the detection of environmental and dietary cytotoxic and genotoxic agents.  $\text{IC}_{50}$  values (median inhibitory concentrations that cause approximately 50% cell death) were: **2**–417; **5**–300; **6**–310; **7**–279  $\mu\text{g}/\text{ml}$  (Fig. 4).

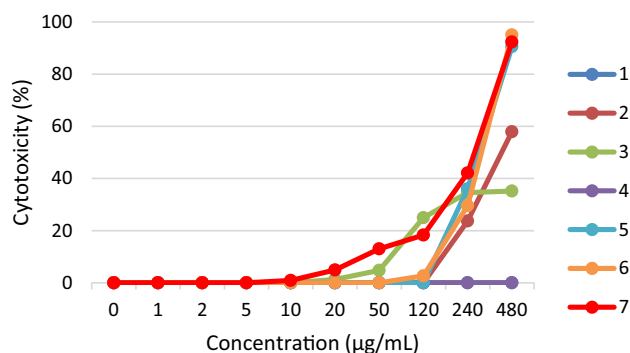


**Fig. 4** The in vitro cytotoxicity results toward the HepG2 cell line at different concentrations of the Schiff's bases (**1–7**)

The experimental results revealed that the nature and position of substituents on the aromatic rings affected the magnitude of cytotoxic activity. Compound **1** bearing an electron-withdrawing nitro group and **4** with mixed electron-withdrawing and electron-donating substituents did not show any cytotoxic activity. The presence of nitro and hydroxy groups made **3** slightly active. Exchanging hydroxy groups for chlorine (**2**) rendered this compound more active, markedly enhancing the cytotoxic activity toward the HepG2 cells. The compounds **5**, **6** and **7**, bearing multiple electron-donating methoxy and hydroxy groups, affected the cell viability in a dose-dependent manner, proving themselves the most active members of this series. Overall, compounds **2**, **3**, **5–7** caused disruptions in the cell cycle of the HepG2 cells. The studied compounds exhibited only mild levels of antiproliferative activity against HepG2 cell line. These preliminary results merit additional investigations. Thus, these compounds will be further studied with a more efficient disease-oriented screening strategy employing various microbial strains, and both normal and tumour human cell lines.

## Conclusions

In conclusion, we have successfully developed a simple one-pot procedure for the synthesis of C–2, N–3 di-substituted quinazolinone derived Schiff's bases. A new catalytic approach using the combined action of reusable heterogeneous PMoA/SiO<sub>2</sub> catalyst and microwave field provides benefits in terms of yields, environmental safety, and operational simplicity. The main advantages of this method include mild reaction conditions, excellent yields, considerably shorter reaction times, and application of a reusable catalyst without significant loss of efficiency over several catalytic cycles. Various spectroscopic methods were used in the structural analysis of these new cytotoxic agents. Furthermore, the examination of the antioxidant capacity of the new compounds by UV–Vis and EPR spectroscopy also contributes to the understanding of the structure–activity relationships of these compounds. The experimental data clearly indicate that significant correlation exists between the molecular structure and the radical scavenging properties. A preliminary cytotoxicity screening against a malignant cell line indicates that compounds **5**, **6** and **7** exhibit dose-dependent cytotoxic activity against HepG2 cells. The studied compounds exhibit only mild antiproliferative effect but significant antioxidant activity. Their structural and physico-chemical properties make these compounds promising candidates for biological, photo-biological, and photochemical experiments, and thus further studies are currently in progress in order to explore their potential.

**Acknowledgements** The authors would like to acknowledge financial support from the Slovak Grant Agency, VEGA Grants No. 2/0100/14, 1/0041/15, 2/0027/16, 2/0022/18 and SP Grant 2003SP200280203 supported by the Research & Development Operational Program funded by the ERDF.

## References

- Berridge MV, Herst PM, Tan AS (2005) Tetrazolium dyes as tools in cell biology: new insights into their cellular reduction. *Biotechnol Ann Rev* 11:127–152. [https://doi.org/10.1016/S1387-2656\(05\)11004-7](https://doi.org/10.1016/S1387-2656(05)11004-7)
- Besson T, Chosson E (2007) Microwave-assisted synthesis of bioactive quinazolines and quinazolinones. *Comb Chem High Throughput Screen* 10:903–917. <https://doi.org/10.2174/138620707783220356>
- Blevins AA, Blanchard GJ (2004) Effect of positional substitution on the optical response of symmetrically disubstituted azobenzene derivatives. *J Phys Chem B* 108:4962–4968. <https://doi.org/10.1021/jp037436w>
- Brees KD, Lamèthe JF, DeArmitt C (2000) Improving synthetic hindered phenol antioxidants: learning from vitamin E. *Polym Degrad Stab* 70:89–96. [https://doi.org/10.1016/S0141-3910\(00\)00094-X](https://doi.org/10.1016/S0141-3910(00)00094-X)
- Chawla A, Batra Ch (2013) Recent advances of quinazolinone derivatives as marker for various biological activities. *Int Res J Pharm* 4:49–58. <https://doi.org/10.7897/2230-8407.04309>
- Cozzi PG (2004) Metal–Salen schiff base complexes in catalysis: practical aspects. *Chem Soc Rev* 33:410–421. <https://doi.org/10.1039/B307853C>
- Crompton EM, Lewis FD (2004) Positional effects of the hydroxy substituent on the photochemical and photophysical behavior of 3- and 4-hydroxystilbene. *Photochem Photobiol Sci* 3:660–668. <https://doi.org/10.1039/b403661a>
- Da Silva CM, Da Silva DL, Modolo LV, Alves RB, De Resende MA, Martins CVB, De Fatima A (2011) Schiff bases: a short review of their antimicrobial activities. *J Adv Res* 2:1–8. <https://doi.org/10.1016/j.jare.2010.05.004>
- Díaz MS, Freile ML, Gutiérrez MI (2009) Solvent effect on the UV/Vis absorption and fluorescence spectroscopic properties of berberine. *Photochem Photobiol Sci* 8:970–974. <https://doi.org/10.1039/b822363g>
- Ernst OP, Lodowski DT, Elstner M, Hegemann P, Brown LS, Kandori H (2014) Microbial and animal rhodopsins: structures, functions, and molecular mechanisms. *Chem Rev* 114:126–163. <https://doi.org/10.1021/r4003769c>
- Firouzabadi H, Jafari AA (2005) Heteropoly acids, their salts and polyoxometalates as heterogenous, efficient and eco-friendly catalysts in organic reactions: Some recent advances. *J Iran Chem Soc* 2:85–114. <https://doi.org/10.1007/BF03247201>
- Fülöp F, Simeonov M, Pihlaja K (1992) Formation of 1,2-dihydroquinazolin-4(3H)-ones. Reinvestigation of a recently reported 1,3,4-benzotriazepine synthesis. *Tetrahedron* 48:531–538. [https://doi.org/10.1016/S0040-4020\(01\)89014-1](https://doi.org/10.1016/S0040-4020(01)89014-1)
- Gawad ANM, Georgey HH, Youssef RM, El-sayed NA (2010) Synthesis and antitumor activity of some 2,3-disubstituted quinazolin-4(3H)-ones and 4,6-disubstituted-1,2,3,4-tetrahydroquinazolin-2H-ones. *Eur J Med Chem* 45:6058–6067. <https://doi.org/10.1016/j.ejmech.2010.10.008>
- Guo Z, Xing R, Liu S, Zhong Z, Ji X, Wang L, Li P (2007) Antifungal properties of Schiff bases of chitosan, N-substituted chitosan and quaternized chitosan. *Carbohydr Res* 342:1329–1332. <https://doi.org/10.1016/j.carres.2007.04.006>
- Halliwell B, Gutteridge JMC (1999) Free radicals in biology and medicine, 3rd edn. Clarendon Press, Oxford

- Hricovíni M, Hricovíni M (2017) Photochemically-induced anti-syn isomerization of quinazolinone-derived Schiff's bases: EPR, NMR and DFT analysis. *Tetrahedron* 73:252–261. <https://doi.org/10.1016/j.tet.2016.12.011>
- Hricovíniová Z (2006) The effect of microwave irradiation on Mo(VI) catalyzed transformations of reducing saccharides. *Carbohydr Res* 341:2131–2134. <https://doi.org/10.1016/j.carres.2006.05.007>
- Hricovíniová Z (2010) A new approach to Amadori ketoses via Mo(VI)-catalyzed stereospecific isomerization of 2-C-branched sugars bearing azido function in a microwave field. *Tetrahedron Asymm* 21:2238–2243. <https://doi.org/10.1016/j.tetasy.2010.07.027>
- Hricovíniová Z (2016) Surfactants of biological origin: the role of MO(VI) and microwaves in the synthesis of xylan-based non-ionic surfactants. *Carbohydr Polym* 144:297–304. <https://doi.org/10.1016/j.carbpol.2016.02.070>
- Kajiyama T, Ohkatsu Y (2001) Effect of para-substitutes of phenolic antioxidants. *Polym Degrad Stab* 71:445–452. [https://doi.org/10.1016/S0141-3910\(00\)00196-8](https://doi.org/10.1016/S0141-3910(00)00196-8)
- Kaur H, Limb SM, Ramasamy K, Vasudevan M, Shah SAA, Narasimhan B (2017) Diazenyl schiff bases: synthesis, spectral analysis, antimicrobial studies and cytotoxic activity on human colorectal carcinoma cell line (HCT-116). *Arab J. Chem.* <https://doi.org/10.1016/j.arabjc.2017.05.004>
- Khan MTH, Khan R, Wuxiuer Y, Arfan M, Ahmed M, Sylte I (2010) Identification of novel quinazolin-4 (3H)-ones as inhibitors of thermolysin, the prototype of the M4 family of proteinases. *Bioorg Med Chem* 18:4317–4327. <https://doi.org/10.1016/j.bmc.2010.04.083>
- Kozhevnikov IV (1998) Catalysis by heteropoly acids and multicomponent polyoxometalates in liquid-phase reactions. *Chem Rev* 98:171–198. <https://doi.org/10.1021/cr960400y>
- Kumar A, Sharma P, Kumari P, Lal Kalal B (2011) Exploration of antimicrobial and antioxidant potential of newly synthesized 2,3-disubstituted quinazolin-4(3H)-ones. *Bioorg Med Chem Lett* 21:4353–4357. <https://doi.org/10.1016/j.bmcl.2011.05.031>
- Kuntikana S, Bhat C, Kongot M, Bhat S, Kumar A (2016) An expeditious green cascade synthesis of 3-Arylideneaminoquinazolin-4(1H)-one derivatives via 'solvent drop grinding' and their antioxidant and dna protective studies. *Chem Select* 1:1723–1728. <https://doi.org/10.1002/slct.201600362>
- Loupy A (2006) *Microwaves in Organic Synthesis*. Wiley-VCH
- Martins MAP, Frizzo CP, Moreira DN, Buriol L, Machado P (2009) Solvent-Free Heterocyclic Synthesis. *Chem Rev* 109:4140–4182. <https://doi.org/10.1021/cr9001098>
- Mhaske SB, Argade NP (2006) The chemistry of recently isolated naturally occurring quinazolinone alkaloids. *Tetrahedron* 62:9787–9826. <https://doi.org/10.1016/j.tet.2006.07.098>
- Michael JP (2005) Quinoline, quinazolinone and acridone alkaloids. *Nat Prod Rep* 22:627–646. <https://doi.org/10.1039/B413750G>
- Mosmann T (1983) Rapid colorimetric assay for cellular growth and survival: application to proliferation and cytotoxicity assays. *J Immunol Methods* 65:55–63. [https://doi.org/10.1016/0022-1759\(83\)90303-4](https://doi.org/10.1016/0022-1759(83)90303-4)
- Nielsen IB, Petersen MÅ, Lammich L, Nielsen MB, Andersen LH (2006) Absorption studies of neutral retinal schiff base chromophores. *J Phys Chem A* 110:12592–12596. <https://doi.org/10.1021/jp064901r>
- Przybylski P, Huczynski A, Pyta K, Brzezinski B, Bartl F (2009) Biological properties of schiff bases and azo derivatives of phenols. *Curr Org Chem* 13:124–148. <https://doi.org/10.2174/138527209787193774>
- Rakesh KP, Manukumar HM, Channe Gowda D (2015) Schiff's bases of quinazolinone derivatives: synthesis and SAR studies of a novel series of potential anti-inflammatory and antioxidants. *Bioorg Med Chem Lett* 25:1072–1077. <https://doi.org/10.1016/j.bmcl.2015.01.010>
- Re R, Pellegrini N, Proteggente A, Pannala A, Yang M, Rice-Evans C (1999) Antioxidant activity applying an improved ABTS radical cation decolorization assay. *Free Radic Biol Med* 26:1231–1237. [https://doi.org/10.1016/S0891-5849\(98\)00315-3](https://doi.org/10.1016/S0891-5849(98)00315-3)
- Sawant VA, Yamgar BA, Sawant SK, Chavan SS (2009) Synthesis, structural characterization, thermal and electrochemical studies of mixed ligand Cu(II) complexes containing 2-phenyl-3-(benzylamino)-1,2-dihydroquinazolin-4-(3H)-one and bidentate N-donor ligands. *Spectrochim Acta Part A* 74:1100–1106. <https://doi.org/10.1016/j.saa.2009.09.015>
- Schiff H (1864) Mittheilungen aus dem Universitätslaboratorium in Pisa: eine neue reihe organischer Basen. *Justus Liebigs Annalen der Chemie* 131:118–119. <https://doi.org/10.1002/jlac.18641310113>
- Sztanke K, Maziarka A, Osinka A, Sztanke M (2013) An insight into synthetic Schiff bases revealing antiproliferative activities in vitro. *Bioorg Med Chem* 21:2648–3666. <https://doi.org/10.1016/j.bmc.2013.04.037>
- Tian X, Schaich KM (2013) Effects of molecular structure on kinetics and dynamics of the trolox equivalent antioxidant capacity Assay with ABTS\*. *J Agric Food Chem* 61:5511–5519. <https://doi.org/10.1021/jf4010725>
- Walker RB, Everette JD (2009) Comparative reaction rates of various antioxidants with ABTS radical cation. *J Agric Food Chem* 57:1156–1161. <https://doi.org/10.1021/jf8026765>
- Wang XS, Sheng J, Lu L, Yang K, Li YL (2011) Combinatorial synthesis of 3-Arylidene aminoquinazolin-4(1H)-one derivatives catalyzed by iodine in ionic liquids. *ACS Combinat Sci* 13:196–199. <https://doi.org/10.1021/co1000713>
- Zahedifard M, Faraj FL, Paydar M, Looi ChY, Hajrezaei M, Hasanpourghadi M, Kamalidehghan B, Majid NA, Ali HM, Abdulla MA (2015) Synthesis, characterization and apoptotic activity of quinazolinone Schiff base derivatives toward MCF-7 cells via intrinsic and extrinsic apoptosis pathways. *Sci Rep* 5(11544):1–17. <https://doi.org/10.1038/srep11544>
- Zhang J, Cheng P, Ma Y, Liu J, Miao Z, Ren D, Fan C, Liang M, Liu L (2016) An efficient nano CuO-catalyzed synthesis and biological evaluation of quinazolinone Schiff base derivatives and bis-2,3-dihydroquinazolin-4(1H)-ones as potent antibacterial agents against *Streptococcus lactis*. *Tetrahedron Lett* 57:5271–5277. <https://doi.org/10.1016/j.tetlet.2016.10.047>
- Zoubi WA (2013) Biological activities of Schiff bases and their complexes: a review of recent works. *Int J Org Chem* 3:73–95. <https://doi.org/10.4236/ijoc.2013.33A008>